Magnetostriction of bismuth in quantizing magnetic fields

J-P. Michenaud
Laboratoire de Physico-Chimie et de Physique de l'État Solide, Université Catholique de Louvain, B-1348 Louvain-la-Neuve, Belgium

J. Heremans
Laboratoire de Physico-Chimie et de Physique de l'État Solide, Université Catholique de Louvain, B-1348 Louvain-la-Neuve, Belgium
and Francis Bitter National Magnet Laboratory, Massachusetts Institute of Technology, Cambridge, Massachusetts 02139

M. Shayegan
Center for Materials Science and Engineering, Massachusetts Institute of Technology, Cambridge, Massachusetts 02139
and Francis Bitter National Magnet Laboratory, Massachusetts Institute of Technology, Cambridge, Massachusetts 02139

C. Haumont
Laboratoire de Physico-Chimie et de Physique de l'État Solide, Université Catholique de Louvain, B-1348 Louvain-la-Neuve, Belgium

(Received 18 January 1982; revised manuscript received 1 June 1982)

Experimental data on the longitudinal magnetostriction of two pure and one p-type bismuth single crystals are reported for fields up to 19 T at temperatures near 2 K. These data are consistent with a model based on the deformation potential concept used to compute the magnetostrictive strain components versus field, using the known field-dependent band structure of bismuth. It is shown that, when elastic and deformation potential constants are available, the magnetostriction of diamagnetic conducting solids can be used as a tool to determine the field-dependent band structure above the ultraquantum limit.

I. INTRODUCTION

Among diamagnetic materials, bismuth exhibits the largest magnetostriction. This property was first meaured by Kapitza[1] above 77 K in pulsed fields up to 25 T, and soon after by Shoenberg[2] in stationary fields of moderate intensity. They analyzed their results in the frame of classical thermodynamics, which leads to a quadratic dependence of the induced strain on the magnetic field. In this approach, the strain tensor components are given by

$$e_{ij}=M_{ijkl}B_kB_l\ . \tag{1}$$

Magnetostriction is thus described by a fourth-rank tensor whose structure is determined by the point group symmetry of Bi. In the usual matrix notation, Eq. (1) becomes

$$\begin{bmatrix} e_1 \\ e_2 \\ e_3 \\ e_4 \\ e_5 \\ e_6 \end{bmatrix} = \begin{bmatrix} m_{11} & m_{12} & m_{13} & m_{14} & 0 & 0 \\ m_{21} & m_{11} & m_{13} & -m_{14} & 0 & 0 \\ m_{31} & m_{31} & m_{33} & 0 & 0 & 0 \\ m_{41} & -m_{41} & 0 & m_{44} & 0 & 0 \\ 0 & 0 & 0 & 0 & m_{44} & 2m_{41} \\ 0 & 0 & 0 & 0 & m_{14} & (m_{11}-m_{12}) \end{bmatrix} \begin{bmatrix} B_1^2 \\ B_2^2 \\ B_3^2 \\ B_2B_3 \\ B_3B_1 \\ B_1B_2 \end{bmatrix} . \tag{2}$$

Kapitza measured only the longitudinal magnetostriction, i.e., the strain parallel to the field, in the trigonal direction and in the perpendicular plane. He found that m_{33} was positive (expansion) and that m_{11} was negative (contraction). The data of Shoenberg, who measured the entire set of m_{ij}, are consistent with Kapitza's results at lower fields.

It is worth noting that the expected quadratic dependence was indeed observed along the trigonal direction, in the field range up to 25 T, while the longitudinal magnetostriction in the perpendicular plane exhibited a more complicated behavior. The quadratic law was only observed below about 1.5 T. This value is very close to the actual onset of the extreme quantum regime for electrons for $\vec{B}$ along the binary direction, when only the $j=0$ Landau level is occupied. This point will be emphasized later.

Three decades later, it was pointed out by Chandrasekhar[3] that low-temperature magnetostriction exhibits de Haas–van Alphen type oscillations. This effect has been measured on Bi (Ref. 4) and on other diamagnetic metals.[5] This renewed interest in magnetostriction was mainly due to the advent of the very sensitive capacitance method for measuring very small displacements.[6] More recently, Michenaud *et al.*[7] reported longitudinal magnetostriction measurements on a bisectrix Bi sample, above the extreme quantum limit in fields up to 5 T. A rough analysis of these results indicated that the magnetostrictive strain varies like the field-induced change in density of low-cyclotron-mass carriers. The approach of these authors was inspired by a simplified model for the magnetostriction of Bi proposed by Keyes.[8] Also, for the semimetal graphite, Heremans *et al.*[9,10] showed that the longitudinal magnetostrictive strain along the c axis is proportional to the change of carrier density with field. The proportionality factor in that case was used to determine a deformation-potential constant. It was further pointed out that magnetostriction is a unique tool to gain experimental insight to the carrier density above the ultraquantum limit.

The aim of this paper is to present new results of high-field longitudinal magnetostriction in bismuth along the binary and trigonal directions, up to 19 T at low temperature. The data are interpreted in the frame of a more complete model, taking into account the specific contributions of electrons and holes, which are of different character, to the magnetostrictive strain.

The paper starts with a theoretical introduction (Sec. II) in which the electronic magnetostriction model developed for multivalley semiconductors is summarized and extended to the case of bismuth. Section III describes the experimental setup and data. In Sec. IV, numerical calculations are presented and experimental and theoretical results are compared. The last section is devoted to the discussion of the results.

II. THEORY

In diamagnetic materials the magnetostriction is due to the charge carriers. From thermodynamic arguments[11] it follows that magnetostriction is directly related to the stress dependence of the magnetic susceptibility. In principle, all diamagnetic solids should exhibit magnetostriction, owing to the volume dependence of the density of states at the Fermi level.

If all carriers belong to a single band, the electronic magnetostriction is very small. However, if many valleys or bands are present, as for semimetals, the magnetostriction is enhanced by the electron-transfer process. Owing to their different magnetic susceptibilities, some bands or valleys will have higher magnetization energies and a strain can be induced, in a magnetic field, in order to shift the valley extrema and redistribute the carriers until minimization of the free energy is reached. This is the main process of magnetostriction in Bi.

To provide a detailed interpretation of the magnetostriction of Bi, we must express explicitly the induced-strain components versus magnetic field, taking into account the overlap between the valence and conduction bands, as well as the multivalley aspect of the conduction band. Although we are mainly concerned with high-field magnetostriction in the quantum limit, we can still follow the outline developed in Ref. 8 for degenerated multivalley semiconductors like Si and Ge in the classical field range. The reason for this is that, in a first step of the calculation, we are looking for an expression of the strain components as a function of carrier-density changes and band-edge shifts, and that the mathematical structure of that expression, owing to its thermodynamic origin, remains the same, whatever the band shape, carrier disperion relation, and field range.

In this approach, the magnetostrictive strain is a linear function of the field-induced changes $\Delta N^{(i)}$ of the carrier densities in bands or valleys, labeled with superscript (i). In a second step of calculation, these $\Delta N^{(i)}$'s may be determined using the well-known band structure of Bi in a magnetic field.

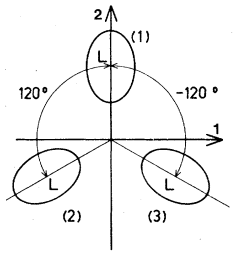

FIG. 1. Identification of the ellipsoids (1), (2), and (3) that represent the L-point electron Fermi surfaces with respect to the binary 1 and bisectrix axis 2. The trigonal axis points out of the paper.

A. Magnetostrictive coupling for Bi

Bi, which belongs to the $\bar{3}m$ point group, is a semimetal containing three electron valleys located at the L points of the Brillouin zone and one hole valley at the T point. The usual crystallographic axes 1,2,3, already implied in Eq. (2), correspond, respectively, to a binary, a bisectrix, and to the trigonal axis. The electron Fermi ellipsoids, labeled (1),(2),(3), are schematically represented in Fig. 1. If electrons only are present, we can simply follow the outline developed by Keyes[8] for n-type Ge and Si.

As the magnetostrictive strain is very small, the electronic free energy $F_e^{(i)}$ of the valley (i) can be found by expanding its statistical expression to the first order in the strain and to the square of the magnetic field, according to Stoner.[12] This expansion gives rise to a coupling term between elastic and magnetic energies, which takes the form

$$\Delta F_e^{(i)}=\Delta N^{(i)}(W_e^{(i)}-\omega)\ , \tag{3}$$

where $W_e^{(i)}$ is the shift of the ith band edge, ω the shift of the Fermi level, and $\Delta N^{(i)}$ the field-induced change of the electronic density. While Eq. (3) has been derived for classical fields,[8] its structure remains in quantum fields. The only difference is that $\Delta N^{(i)}$ no longer varies as B^2. It is worth emphasizing that, in this case, the effect of field is to redistribute the electrons in the different valleys, without changing the total density:

$$\sum \Delta N^{(i)}=0\ . \tag{4}$$

The total coupling term is given by

$$\Delta F_e=\sum_{i=1}^{3}\Delta F_e^{(i)}\ , \tag{5}$$

and the component of the free energy to be minimized for calculating the strain is then

$$\Delta F=F_{\text{elastic}}+\sum_{i=1}^{3}\Delta N^{(i)}(W^{(i)}-\omega)\ . \tag{6}$$

The actual situation for Bi is more complicated, owing to the presence of the band overlap. Two different processes of diamagnetic magnetostriction must now be considered. In high magnetic field, the crystal will be strained not only by the electron-transfer process, already mentioned above, but also by the induced shift W_h of the hole band edge which involves net changes, ΔN and ΔP, of electron and hole densities. From the neutrality condition $\Delta N=\Delta P$, we have

$$\sum_{i=1}^{3}\Delta N^{(i)}=\Delta P\ , \tag{7}$$

where $\Delta N^{(i)}$ represents now the total change of electronic density in the ith valley, in the equilibrium state.

These quantities are functions of the deformation-potential constants and the strain components. In order to compute the strain components versus magnetic field, we must minimize the coupling term with respect to the strain:

$$\Delta F=F_{\text{elastic}}+\sum_{i=1}^{3}\Delta N^{(i)}(W_e^{(i)}-\omega)$$
$$+\Delta P(W_h+\omega)\ ,$$

or

$$\Delta F=F_{\text{elastic}}+\sum_{i=1}^{3}\Delta N^{(i)}W_e^{(i)}+\Delta P W_h\ . \tag{8}$$

B. The band-edge shifts of Bi

Assuming the validity of the deformation-potential theory originally introduced by Bardeen and Shockley,[13] the shifts $W_e^{(i)}$ and W_h may be related to the strain component e_{kl} (tensorial notation) by

$$W_e^{(i)}=L_{kl}^{(i)}e_{kl} \tag{9}$$

and

$$W_h=T_{kl}e_{kl}\ , \tag{10}$$

where the $L_{kl}^{(i)}$ are the components of the deformation-potential tensor of the ith electronic valley and T_{kl} the similar components for the hole band.

Taking into account the 120° layout of the elec-

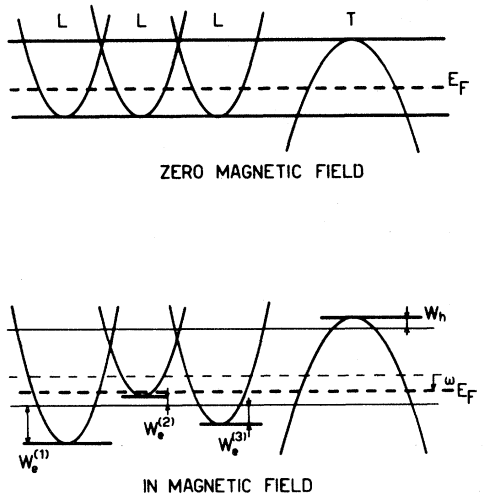

FIG. 2. Schematic representation of the edges' shifts of electron and hole bands in bismuth. The upper schema is relative to the zero-field situation, while the lower one represents the actual situation in magnetic field. The magnitude of the quantities $W_e^{(i)}$ and W_h depend both on field intensity and orientation.

tron Fermi ellipsoids and the tilt angle of the principal axis in the mirror planes of the Brillouin zone (the latter being responsible for the nondiagonal component L_{23}), we get[14]

$$W_e^{(1)}=L_{11}e_{11}+L_{22}e_{22}+L_{33}e_{33}+2L_{23}e_{23}\ , \tag{11}$$

$$W_e^{(2,3)}=\tfrac{1}{4}(L_{11}+3L_{22})e_{11}+\tfrac{1}{4}(3L_{11}+L_{22})e_{22}+L_{33}e_{33}\pm\frac{\sqrt{3}}{2}(L_{11}-L_{22})e_{12}\pm\sqrt{3}L_{23}e_{13}-L_{23}e_{23}\ ,$$

where the upper sign refers to $W_e^{(2)}$, and

$$W_h=T_{11}(e_{11}+e_{22})+T_{33}e_{33} \tag{12}$$

for holes. Figure 2 illustrates schematically the shifts of the band edges.

C. The Bi magnetostrictive strain

The detailed expression of F_{elastic} is given by

$$F_{\text{elastic}}=C_{11}(\tfrac{1}{2}e_{11}^2+\tfrac{1}{2}e_{22}^2+e_{12}^2)+C_{12}(e_{11}e_{22}-e_{12}^2)+2C_{44}(e_{13}^2+e_{23}^2)+C_{14}(2e_{11}e_{23}+4e_{12}e_{13}-2e_{22}e_{23})+C_{13}(e_{11}+e_{22})e_{33}+\tfrac{1}{2}C_{33}e_{33}^2 \tag{13}$$

for the $\bar{3}m$ symmetry of Bi, where the C_{ij} are the elastic constants in matrix notation, and the e_{ij}, the strain components in tensorial notation. Taking into account expressions (9) and (10), the minimization of (8) yields the following relations:

$$\begin{aligned}
e_{11}&=-a\Delta-b\Delta N\ ,\\
e_{22}&=a\Delta-b\Delta N\ ,\\
e_{33}&=-c\Delta N\ ,\\
e_{12}&=-\frac{\sqrt{3}}{2}a(\Delta N^{(2)}-\Delta N^{(3)})\ ,\\
e_{13}&=-\frac{\sqrt{3}}{4}d(\Delta N^{(2)}-\Delta N^{(3)})\ ,\\
e_{23}&=-\tfrac{1}{2}d\Delta\ ,
\end{aligned} \tag{14}$$

where

$$\Delta=\Delta N^{(1)}-\frac{\Delta N^{(2)}+\Delta N^{(3)}}{2} \tag{15}$$

and the coefficients a,b,c,d are given by

$$\begin{aligned}
a&=(s_{11}-s_{12})\left[\frac{L_{11}-L_{22}}{2}\right]+s_{14}L_{23}\ ,\\
b&=\left[\frac{s_{11}+s_{12}}{2}\right](L_{11}+L_{22}+2T_{11})+s_{13}(T_{33}+L_{33})\ ,\\
c&=s_{13}(L_{11}+L_{22}+2T_{11})+s_{33}(T_{33}+L_{33})\ ,\\
d&=s_{14}(L_{11}-L_{22})+s_{44}L_{23}\ .
\end{aligned} \tag{16}$$

In (16), the parameters s_{ij} are the elastic compliances of Bi. At this stage, it is worth emphasizing some interesting features:

(i) The shear strain components e_{12} and e_{13} vanish when $\Delta N^{(2)}$ equals $\Delta N^{(3)}$. Owing to the symmetry of the Bi Fermi surface one can already guess that $\Delta N^{(2)}=\Delta N^{(3)}$ when the magnetic field lies in the binary or bisectrix direction. However, in these situations e_{23} does not vanish.

(ii) The strain e_{23} is zero when all $\Delta N^{(i)}$ are equal, i.e., when the magnetic field is parallel to the trigonal axis. In this case all shear components vanish.

(iii) The quantity $\Delta N^{(2)}-\Delta N^{(3)}$ is only due to the electron-transfer process between the electron pockets, independently of the overlap change, while the

quantity Δ depends on both multivalley and overlap processes.

III. EXPERIMENTAL SETUP AND RESULTS

The longitudinal magnetostriction of two 99.9999%-pure bismuth samples and one tin-doped bismuth sample have been measured by the capacitance method.[6] The bismuth samples were single crystals whose length was along the binary and trigonal direction, respectively. The tin-doped sample (Bi 56, as numbered in Refs. 15 and 16) is a bisectrix rod containing 27×10^{17} atoms cm^{-2} Sn. Since Sn acts as a monovalent acceptor,[15] one may calculate[16] that this Bi 56 sample has its Fermi level within the energy gap at the L point and thus only T holes are present at low temperature.

The capacitance cell, made of beryllium copper, has been developed from a design of Brändli and Griessen.[17] It can contain samples of various lengths. Two hemispheres are glued to the sample ends, in such a way that the sample may rotate freely should a torque strain component develop due to a misalignment in field. We verified by x-ray fluorescence that the material used contained no more than a few parts per thousand cobalt or other magnetic impurities.

The experiment was carried out with the cell immersed in superfluid helium to guarantee thermal stability. The field was applied along the longitudinal axis of the sample and cell by means of a water-cooled Bitter magnet. The capacitance between the electrodes was measured by means of a General Radio 1615 bridge with a lock-in voltmeter as detector. The bridge was balanced at zero field. Then the field was swept (1—10 T/min) and the deviation of the lock in recorded versus field. It was verified that this deviation is proportional to the change in capacitance. The magnetostrictive strain was hence computed from this deviation.

The plain curves in Fig. 3 and 4 represent, respectively, the measured longitudinal strain $e_{11}(B_1)$ and $e_{33}(B_3)$ versus field up to 19 T. Each experimental curve exhibits the expected oscillatory behavior, associated with the de Haas-van Alphen effect, in the low-field range, followed by a monotonic dependence in the extreme quantum range. In Fig. 5, the flat solid line represents the strain $e_{22}(B_2)$ measured on the Bi 56 sample, while the lower solid line is the corresponding $e_{22}(B_2)$ for a pure Bi sample up to 5 T at 4 K taken from Ref. 7. We notice that, for pure Bi, if we exclude the oscillatory range, e_{11} and e_{22} are negative while e_{33} is positive, in accordance with Kapitza's results at higher temperatures.

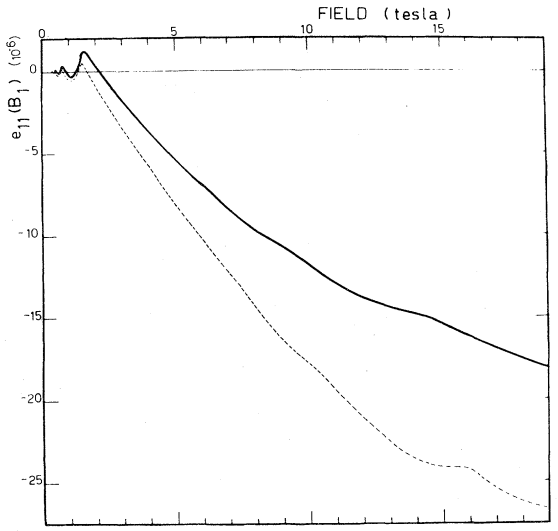

FIG. 3. Longitudinal magnetostrictive strain $e_{11}(B_1)$ along the binary axis vs magnetic field at 1.3 K. Note that the strain is negative over most of the field range. The solid line is the experimental results; the dashed line has been calculated according to Eqs. (14).

IV. DISCUSSION

Since all the values entering in Eqs. (14)—(16) are known at least approximately, it has been possible to compute the values of $e_{11}(B_1)$, $e_{22}(B_2)$, and $e_{33}(B_3)$, and compare them to the observed magnetostriction curves, *without using any adjustable parameter.* The first step is to calculate the carrier-density changes $\Delta N^{(i)}$ in a magnetic field in the limit of absolute zero temperature. To do this we use the field-dependent electron band structure of bismuth, about which more details will be given later. For the T-point holes, we assume a simple parabolic dispersion relation that splits up into equally spaced Landau levels. From those band

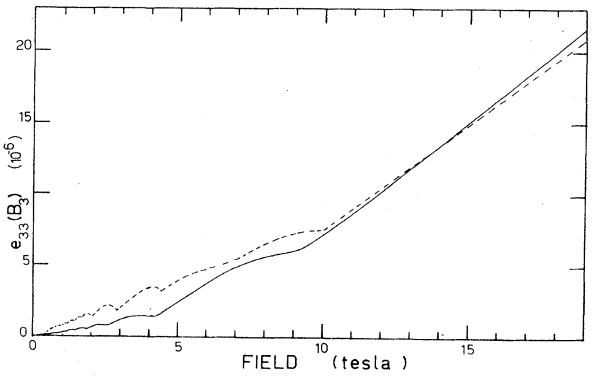

FIG. 4. Calculated (dashed line) and measured (solid line) longitudinal magnetostriction along the trigonal axis $e_{33}(B_3)$ of pure bismuth vs magnetic field at 1.3 K.

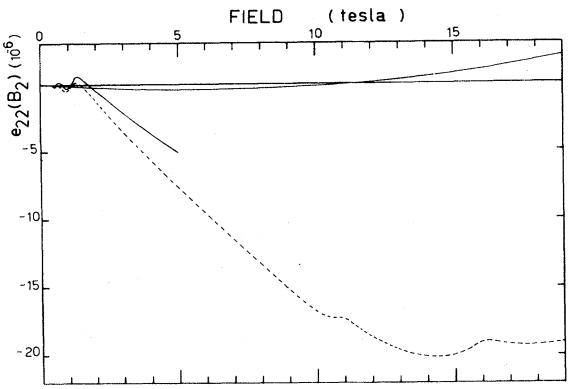

FIG. 5. Longitudinal magnetostrictive strain $e_{22}(B_2)$ along the bisectrix axis. The dashed curve is the strain for pure bismuth, calculated according to Eqs. (14); over most of the range, it is negative. The solid curve that stops at 5 T represents $e_{22}(B_2)$, as measured by Michenaud *et al.* (Ref. 7) on pure bismuth. The flat solid curve near the zero ordinate represents the strain measured at 1.3 K on a Sn-doped sample with 27×10^{17} cm^{-3} excess hole density. Such a sample has only one type of carrier and exhibits a very small magnetostriction.

structures, we calculate the densities of electron and hole states. To get the Fermi level and the carrier densities in each band and pocket, we impose the neutrality condition, which for pure bismuth reads

$$P=\sum_i N^{(i)}\,, \tag{17}$$

and for tin-doped bismuth with an excess hole density D,

$$P-D=\sum_i N^{(i)}\,. \tag{18}$$

The details of the calculations are based on the following choices for the parameters of the electron bands:

(1) We use the effective mass tensor of Dinger and Lawson.[18]

(2) When the field is applied in the bisectrix or binary directions, and is such that only the $j=0$ Landau level is populated (the ultraquantum regime), the refined model of Vecchi *et al.*[19] is used, but with the effective masses of Dinger and Lawson[18] for the sake of consistency. Nevertheless, it may be easily calculated[20] that the masses of Ref. 18 are consistent, within the quoted experimental errors, with the results of Ref. 19.

TABLE I. Deformation-potential constants, measured from magnetoacoustic attenuation (units of eV).

$L_{11}=-2.2$	$L_{33}=-1.7$
$L_{22}=5.9$	$T_{11}=1.2$
$L_{23}=1.5$	$T_{33}=-1.2$

(3) When the field is applied in the trigonal direction, a simple model, the Lax model, has been shown by Maltz and Dresselhaus[21] to describe their magnetoreflection experiments quite well, and has therefore been used here.

Two other sets of parameters are required in Eq. (16): the elastic constants and the deformation potentials. For the former, we used the values reported at 4.2 K by Eckstein *et al.*[22] The deformation-potential constants of Bi have been measured from magnetoacoustic attenuation by Walther,[23] whose results are summarized in Table I.

The results of the calculations for pure Bi are shown in Figs. 3, 4, and 5 as dashed curves for $e_{11}(B_1)$, $e_{33}(B_3)$, and $e_{22}(B_2)$, respectively. For the Sn-doped sample, it has been numerically verified that as expected no carrier-density change or electronic magnetostriction occurs at any field. The same calculations yield information on the other components of the magnetostrictive strain tensor of bismuth. These as well as the field-dependent carrier densities at four selected values of the magnetic field in the binary, bisectrix, and trigonal direction are summarized in Table II. Comparison of the calculated and experimental curves in Figs. 3–5 shows differences of the order of 7% in the position of the quantum oscillations extrema with respect to field.

The difference in magnitude between calculated and measured strain components e_{11} and e_{22} can be ascribed to large uncertainties in the values given in Table I. See, for example, Katsuki.[24] These components, in contrast to e_{33}, depend on the shear deformation potential L_{23} for which only one experimental value is known. We have noticed that a reversal of sign of L_{23} gives a complete agreement in magnitude. As we cannot justify this in view of Walther's[25] discussion, we take it to be probably accidental.

Magnetostriction is weakly dependent on temperature as observed in the early work of Kapitza. While no experimental data between 4.2 and 77 K are available, it is possible in a tentative approach to connect low- and high-temperature results by means of the empirical dependence of m_{11} [see Eq. (2)] on temperature (in units of T^{-2}):

$$m_{11}(T)-=12.25(1-2.4\times10^{-3}T)10^{-8} \tag{19}$$

found by Kapitza for $77<T<300$ K and below 1.5 T, where the strain has a quadratic field dependence. Assuming that Eq. (19) can be extrapolated

TABLE II. Calculated carrier densities (in 10^{17} cm^{-3}) and magnetostrictive strain components ($\times 10^6$) for several values and directions of the magnetic field.

Field direction	Binary field				Bisectrix field				Trigonal field			
Field intensity (T)	5	10	15	20	5	10	15	20	5	10	15	20
$N^{(1)}$	0.573	0.257	0.33	0.30	3.00	5.50	6.37	5.95	1.41	1.85	2.78	3.71
$N^{(2)}=N^{(3)}$	2.47	4.40	5.70	6.29	1.36	2.29	3.12	3.76	1.41	1.85	2.78	3.71
e_{11}	−7.97	−17.7	−23.9	−26.6	0.166	−1.50	−4.54	−8.12	−1.88	−3.53	−6.95	−10.4
e_{22}	1.02	1.97	1.58	1.10	−7.63	−16.8	−20.0	−18.5	−1.88	−3.53	−6.95	−10.4
e_{33}	7.44	16.9	23.9	27.4	8.00	19.6	26.3	28.6	4.04	7.57	14.9	22.3
e_{12}	0	0	0	0	0	0	0	0	0	0	0	0
e_{13}	0	0	0	0	0	0	0	0	0	0	0	0
e_{23}	4.71	10.3	13.3	14.5	−4.08	−7.98	−8.08	−5.45	0	0	0	0

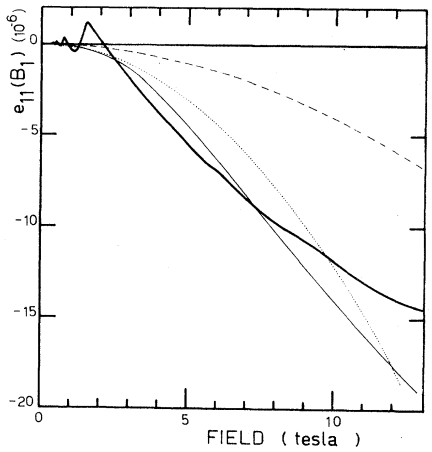

FIG. 6. Comparison between high- and low-temperature magnetostriction. The thick solid line represents the longitudinal magnetostriction along the binary direction at 2 K and the dashed line the corresponding steady magnetostriction calculated from the extrapolated relation (20). The thin solid line represents the longitudinal magnetostriction in the basal plane measured by Kapitza at 83 K, and the dotted line is the calculated steady magnetostriction at the same temperature, according the empirical equation (19). A good fit is only observed below 1.5 T.

to 2 K, we get

$$e_{11}(H_1)=12.2\times 10^{-8}H_1^2 \ . \tag{20}$$

Equation (20) should correspond to a quadratic or steady magnetostriction term which must prevail below the quantizing fields at liquid helium. Unfortunately, it cannot be verified experimentally at low fields owing to the smallness of the effect. At higher fields, the calculated function (20) lies between the envelopes of the extrema of the oscillatory magnetostriction, as shown in Fig. 6. This fact suggests that the extrapolation of Eq. (20) is permissible and gives the right order of magnitude of the steady magnetostriction at low temperatures. With increasing temperature, because of the thermal smearing of the energy levels involved, the oscillations of the $\Delta N^{(i)}$ and thus of the strain components decrease and vanish, as is the case for the de Haas–van Alphen effect. Only the steady magnetostriction survives. The departure at 77 K from the expected quadratic behavior, which remained unexplained by Kapitza, is mainly due to the quantization of the energy levels and the occurrence of the ultraquantum limit, above which electrons are collected in the single $j=0$ level.[19] While oscillations disappear in the thermal smear, at sufficiently high temperature and at moderate quantum field, in

the extreme quantum range, magnetostriction remains under quantum influence and the strain still follows the monotonic changes of carrier densities. This effect is most pronounced when the field lies in the basal plane because of the low electronic cyclotron masses. When $\vec{B}$ is along the trigonal direction, the cyclotron masses are greater and no trace of quantum effects subsists above 77 K, leading to a classical magnetostriction as observed by Kapitza.

V. CONCLUSION

The above model of magnetostriction is in a reasonable agreement with the experimental data on Bi. It confirms the high-field electronic band structure as developed by Vecchi *et al.*[19] The model also includes the role of donors or acceptors in magnetostriction. Our experiment on one Sn-doped bismuth sample, which only contains holes at low temperature, clearly revealed tiny magnetostriction. One can also infer that, at low temperature, a Te-doped Bi sample in which only electrons are present should exhibit no longitudinal magnetostriction along the trigonal axis, due to the electron-transfer process.

A last comment concerns transport properties in a magnetic field. As pointed out by Keyes,[8] magnetostriction is by itself a cause of magnetoresistance, owing to the electron transfer between valleys of different mobilities. The usual analysis of transport properties in a magnetic field does not take this effect into account. Also, as quantum effects can be detected for some field directions even at high temperature, the structure of the transport tensors as derived by Akgöz and Saunders[25,26] for classical fields could occasionally not be suitable.

ACKNOWLEDGMENTS

The authors are much indebted to P. Coopmans, who built the measurement cell and to Dr. L. Rubin and B. Brandt for technical assistance. They enjoyed useful discussions with Professor J-P. Issi, Professor M. S. Dresselhaus, Professor F. J. Blatt, Professor R. Griessen, and Dr. G. Dresselhaus. One of us (M.S.) acknowledges support from AFOSR Grant No. F 49620-81-C-0006. J.H. is supported by the Fonds National Belge de la Recherche Scientifique. The work of J.H. and M.S. at FBNML was supported by the National Science Foundation, and the work of C.H. was supported by a grant from the Institut pour la Recherche Scientifique dans l'Industrie et l'Agriculture (Brussels, Belgium).

[1]P. Kapitza, Proc. R. Soc. London Ser. A 135, 568 (1932).
[2]D. Shoenberg, Proc. R. Soc. London Ser. A 150, 619 (1935).
[3]B. S. Chandrasekhar, Phys. Lett. 6, 27 (1963).
[4]B. A. Green and B. S. Chandrasekhar, Phys. Rev. Lett. 11, 331 (1963); also T. Nakajima (private communication).
[5]See, for example the review article of B. S. Chandrasekhar and E. Fawcett, Adv. Phys. 20, 775 (1971).
[6]G. K. White, Cryogenics 1, 151 (1961).
[7]J-P. Michenaud, J. Heremans, J. Boxus, and C. Haumont, J. Phys. C 14, L13 (1981).
[8]R. W. Keyes, in *Solid State Physics,* edited by H. Ehrenreich, F. Seitz, and D. Turnbull (Academic, New York, 1967), Vol. 20, p. 37.
[9]J. Heremans, J-P. Michenaud, M. Shayegan, and G. Dresselhaus, J. Phys. C 14, 3541 (1981).
[10]J. Heremans, J-P. Michenaud, C. Haumont, M. Shayegan, and G. Dresselhaus, in 15th Biennial Conference on Carbon, Philadelphia, 1981 (unpublished).
[11]P. Kapitza, Proc. R. Soc. London Ser. A 135, 537 (1932).
[12]E. C. Stoner, Proc. R. Soc. London Ser. A 152, 672 (1935).
[13]J. Bardeen and W. Shockley, Phys. Rev. 80, 72 (1950).
[14]A. J. Lichnowski and G. A. Saunders, J. Phys. C 10, 3243 (1977).
[15]J. M. Noothoven van Goor, Philips Res. Rep. Suppl. 4 (1971).
[16]J. Heremans, Ph.D. thesis, University of Louvain, 1978 (unpublished).
[17]G. Brändli and R. Griessen, Cryogenics 13, 3541 (1973).
[18]R. J. Dinger and A. W. Lawson, Phys. Rev. B 12, 5215 (1973).
[19]M. P. Vecchi, J. R. Pereira, and M. S. Dresselhaus, Phys. Rev. B 14, 298 (1976).
[20]O. P. Hansen (private communication); see also Ref. 16.
[21]M. Maltz and M. S. Dresselhaus, Phys. Rev. B 2, 2877 (1970).
[22]Y. Eckstein, A. W. Lawson, and D. H. Renecker, J. Appl. Phys. 31, 1534 (1960).
[23]K. Walther, Phys. Rev. 174, 782 (1968).
[24]S. Katsuki, J. Phys. Soc. Jpn. 26, 696 (1969).
[25]Y. C. Akgöz and G. A. Saunders, J. Phys. C 8, 1387 (1975).
[26]Y. C. Akgöz and G. A. Saunders, J. Phys. C 8, 2962 (1975).